A Real-Time Range-Adaptive Impedance Matching Utilizing a Machine Learning Strategy Based on Neural Networks for Wireless Power Transfer Systems

Soyeon Jeong, *Student Member, IEEE*, Tong-Hong Lin, *Graduate Student Member, IEEE*, and Manos M. Tentzeris, *Fellow, IEEE*

***Abstract*— In this article, the implementation of a machine learning (ML) strategy based on neural networks for the real-time range-adaptive automatic impedance matching of wireless power transfer (WPT) applications is discussed. This approach for the effective prediction of the optimal parameters of the tunable matching network and the selection of range-adaptive transmitter coils (Tx) is introduced in this article, aiming to achieve an effective automatic impedance matching over a wide range of relative distances. We propose a WPT system consisting of a tunable matching circuit and three Tx coils that have different radii and are simultaneously controlled by trained neural network models, returning an output set of matching capacitances as well as the optimal single transmitter among the three transmitters. In addition, a proof-of-concept prototype of the entire real-time range-adaptive automatic impedance-matching system is built and characterized. Finally, the proposed approach achieves a power transfer efficiency (PTE) of around 90% for ranges within 10–25 cm.**

***Index Terms*— Automatic impedance matching, machine learning (ML), neural network, resonant coupling, wireless power transfer (WPT).**

I. Introduction

THE real-time impedance matching of wireless power transfer (WPT) systems using magnetic resonance coupling (MRC) has become a critical challenge in order to maintain a reasonable power transfer efficiency (PTE) for time-varying configurations. Various MRC system architectures are used in the near-field WPT, which can facilitate the impedance matching to optimize the system transfer characteristics. At this point, the frequency-splitting phenomenon is a key issue that typically happens in multi-coil systems, such as multi-relay coils, multi-transmitter coils, and multi-receiver coils, related to the PTE and capability of the WPT system. In other words, there will be an impedance mismatch between the resonator impedance and the load impedance by changing the distance, changing the orientation, or introducing any generic misalignment. To overcome this issue, the adaptive frequency tracking [1], [2] approach has been used, which can achieve maximum power delivery, but only operating in a wide bandwidth that is typically outside the narrow industrial, scientific, and medical regulated bands. As the importance of robustness against distance variation in WPT systems becomes greater, Duong and Lee [3] and Lee *et al.* [4] proposed an impedance-matching technique by changing the distance between multiple coils physically. By adjusting the relative distances or angles between adjacent coils based on the optimal coupling factor between the source and the internal resonator [3], a high-efficiency WPT system is achieved without any lossy matching network. This adaptive system [4] with the reconfigurable resonant coil configuration consists of a series of subcoils that use switches to control the number of turned-on subcoils increasing the efficient transfer range. Similarly, an analytic design method for impedance-matched WPT systems using an arbitrary number of coils by applying flexible coil positioning has been proposed in [5]. Moreover, Qiu *et al.* [6] recently proposed digital programmable transmitter coils to maximize the system efficiency in the WPT systems when a receiver coil is given. In [7] and [8], a tunable matching circuit was designed for a range-adaptive WPT system with switching capacitors to obtain wide tunability from the impedance-matching circuit. When the input impedance of a WPT system changes with the distance, a tunable matching circuit can be used to match the variable impedance with the distance. The L-type or inverted L-type matching network in the transmitter side is used in [7], and the π-type network in both transmitter and receiver sides is used in [8] with different numbers of relays, inductors, and capacitors for switching. In addition, a range-adaptive WPT system utilizing the multi-loop topology uses a tunable matching network composed of varactors in [9]. In a previously reported work, Bito *et al.* [10] utilized the genetic algorithm (GA) to optimize the matching circuit design over a wide range of impedances to match, and therefore, WPT efficiency is potentially high. Recently, an automatic impedance-matching technique based on the feedforward-backpropagation (BP) neural network has

Manuscript received May 7, 2019; revised August 7, 2019; accepted August 17, 2019. Date of publication September 13, 2019; date of current version December 27, 2019. This article is an expanded version from the IEEE MTT-S International Microwave Symposium (IMS 2019), Boston, MA, USA, June 2–7, 2019. *(Corresponding author: Soyeon Jeong.)*

The authors are with the School of Electrical and Computer Engineering, Georgia Institute of Technology, Atlanta, GA 30332-250 USA (e-mail: sjeong47@gatech.edu).

Color versions of one or more of the figures in this article are available online at http://ieeexplore.ieee.org.

Digital Object Identifier 10.1109/TMTT.2019.2938753

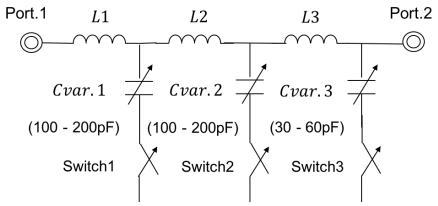

Fig. 1. Simplified schematic of the automatic matching circuit.

been proposed [11] to maintain a PTE at a reasonable level. However, these previously reported systems are limited in the effective ranges of impedances because of their typically unexpected variations of the transfer distance or load impedance. Here, we propose an alternative approach that takes advantage of a novel method based on a feedforward neural network combined with pattern recognition techniques, thus addressing the shortcomings of the aforementioned impedance-matching approaches while retaining high PTE. As a proof of concept, one receiver coil, three selective transmitter coils, and a matching circuit with tunable capacitors are first designed and measured. Then, a machine learning (ML) approach utilizing neural network algorithms that can construct the mapping relationship is presented to improve the power transfer capability of the WPT system. Furthermore, the implementation of an entire real-time range-adaptive impedance-matching circuit and its verification are discussed in detail as an extension of previously reported results [12].

II. WPT Application

A. Matching Circuit Design and Fabrication

A matching circuit topology consisting of three consecutive L-type series inductors and shunt capacitors with a p-i-n diode switch was used in [10]. The simplified schematic of this matching circuit is shown in Fig. 1. To overcome the limited capability of this static topology to provide an acceptable PTE over a wide range of transmitter–receiver distances, one variable capacitor from Murata electronics is employed in this article enabling superior characteristic of the matching circuit compared with previous work and allowing for the on-demand value tuning utilizing the results from the proposed ML approach. These tunable capacitors typically achieve capacitance values that can vary by applying voltage to their electrodes in the range of 100–200 pF (0–5 V) for Cvar.1 and Cvar.2, and 30–60 pF (0–3 V) for Cvar.3 and operate appropriately at 13.56 MHz with the limited range of values. To determine the optimal matching circuit topology with those tunable capacitors, the impedance-matching coverage of multiple topologies, and a π-type and an L-type of multiple sections (one to three consecutive stages) with each section comprising of a series inductor, a shunt capacitor, and a switch were simulated with respective matching impedance coverage ranges shown in Fig. 2, as the verification of the impedance-matching coverage for a variability of the used capacitance values of Cvar.1 (100–200 pF), Cvar.2 (100–200 pF), and Cvar.3 (30–60 pF) in steps of 10 pF. In addition, the reason for using 10-pF steps of the capacitance values is to satisfy the practical control module constraints in a system implementation.

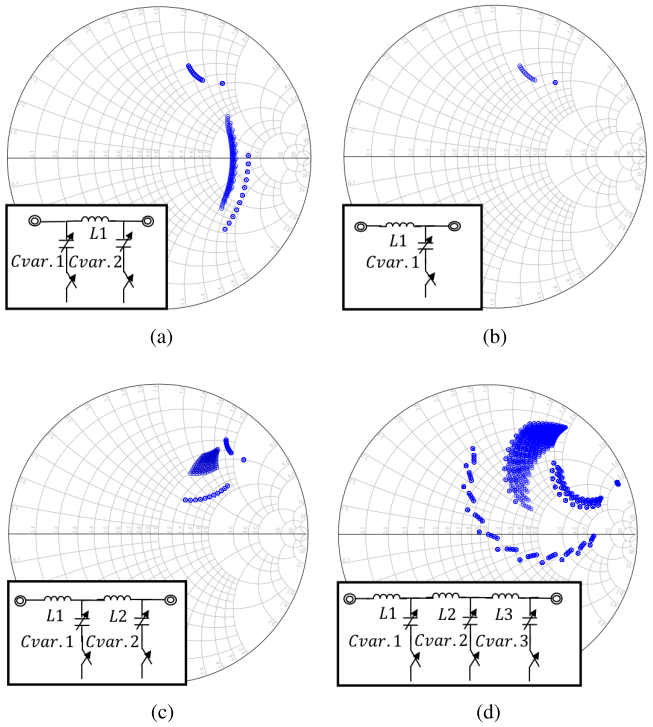

Fig. 2. (a) Simulated input impedance values of π-type matching circuit with Cvar.1 and Cvar.2. (b) Simulated input impedance values of one L-type matching circuit with Cvar.1. (c) Simulated input impedance values of two L-type matching circuits with Cvar.1 and Cvar.2. (d) Simulated input impedance values of three L-type matching circuits with Cvar.1, Cvar.2, and Cvar.3.

Since the power transfer to the load can be maximized when the input impedance of the matching circuit looking from port.2 (Z_{22}) in Fig. 1 is the complex conjugate of the Rx–Tx coil topology impedance input (Z_c), each fixed inductor value of $L1$, $L2$, and $L3$, and the use of the capacitor among Cvar.1, Cvar.2, and Cvar.3 were first optimized to minimize the reflection coefficient $\Gamma = (Z_c^* - Z_{22})/(Z_c^* + Z_{22})$ from the simulated coil configuration (Rx–Tx1, Rx–Tx2, and Rx–Tx3) impedance value (Z_c) distances at 10, 15, and 20 cm. The three consecutive-stage L-type topology was chosen to provide wide impedance-matching coverage and satisfy the practical constraints such as the loss associated with the lumped circuit components. With this proposed method, a wide range of impedance coverage can be realized though the variation in the input impedance Z_{in}. For the inductance values of $L1$, $L2$, and $L3$, the fixed inductor values of 1432, 610, and 1484 nH were optimized corresponding to the values of capacitance's tunable ranges in simulations utilizing advanced design system (ADS) 2016. For the fabrication of a proof-of-concept prototype of the matching circuit, a 1.5-mm-thick substrate from RO4003C provided by the Rogers Cooperation and the inductors with fixed values of 1500 and 560 nH provided by the Coilcraft 0603HL series were used.

B. Receiver and Selective Transmitters Configurations

Both receiver and transmitter coils are open-type helical coils that have a self-resonance frequency of 13.56 MHz. For the proof-of-concept purpose, each coil was designed with

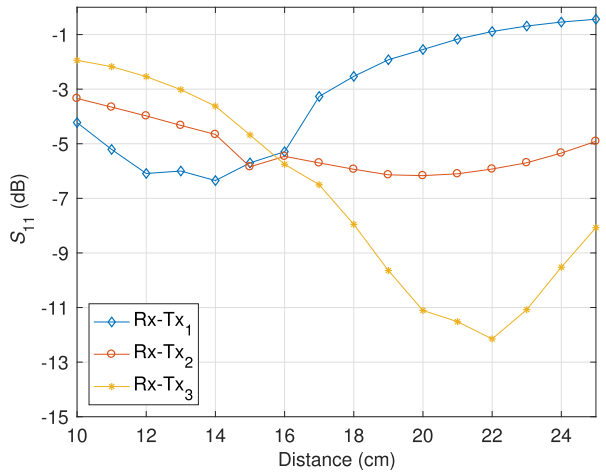

Fig. 3. Simulated reflection coefficient (S_{11}) with respect to Rx–Tx distances.

TABLE I
PARAMETERS OF THE RX AND TX COILS FOR THE PROPOSED WPT SYSTEM

	Receiver	Transmitters		
	Rx	Tx1	Tx2	Tx3
Self-resonance Frequency (MHz)	13.56			
Copper Wire Radius (mm)	0.5			
Radius (cm)	5	10	15	20
Number of turns	27	10	6	4.5
Pitch (mm)	2			

fixed radius values ($r = 5$ cm for the receiver, and 10, 15, and 20 cm for the transmitter coils) to resonate at the same frequency by optimizing the number of turns and the intercoil distance as derived using CST Studio 2016 using the integral solver. A multi-coil transmitter topology was employed to reduce the variation in the input impedance of the WPT system with respect to the distance. To maximize the coil-to-coil efficiency, it was found that the optimal radius of Tx should be approximately equal to the distance of coil-to-coil in [6] according to the following analytically derived equation:

$$r_{\mathrm{Tx}} = d \tag{1}$$

when $r_{Rx} \ll r_{\mathrm{Tx}}$. Based on a detailed design analysis, the overall geometrical design for the Rx and Tx coils is controlled by the key parameters summarized in Table I. To improve the robustness of both the Tx and Rx coil structures, laser cut acrylic boards were use as support fixtures. The extracted S-parameters from the simulations will serve a standard data set for the neural network training presented in Section III-B. A photograph of the fabricated Rx and Tx three-coil prototypes is shown in Fig. 4. Each switch introduces a selectivity of a specific transmitter coil by utilizing a relay, TQ2-L2-4.5V from Panasonic Electric works, featuring a resistance lower than 50 mΩ in the "ON' state. To confirm the effectiveness of this approach, the reflection coefficient (S_{11}) values were simulated according to the coil-to-coil (Rx–Tx1, Rx–Tx2, and Rx–Tx3) distance at 10–25 cm, as shown in Fig. 3, and 10 cm was the minimum possible center-to-center separation distance

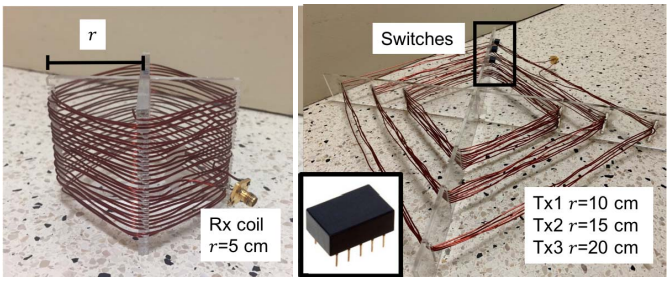

(a) (b)

Fig. 4. (a) Fabricated Rx coil. (b) Fabricated 3-coil Tx with switches.

between the Rx–Tx coils, since the thickness of the support fixtures is 10 cm for Rx and 8 cm for Tx coils. The multi transmitter coil topology can be effectively used in the range-adaptive WPT system in addition to the use of the proposed tunable matching circuit.

III. ML APPROACHI

Neural networks represent powerful ML-based techniques, inspired by the neurons in the human brain, that are designed to recognize patterns or underlying relationships in a set of data. Their networks have turned out to be well suited to modeling high-level abstractions across a wide array of disciplines and industries. The MATLAB neural network toolbox was used to implement suitable neural networks with optimal structure parameters.

A. Optimize the Hyperparameters of the Neural Network

In ML, the hyperparameters are the variables that determine the network structures and the method by which the network is trained. Neural networks can have many hyperparameters that are usually set before the training process, such as the number of hidden layers, the number of epochs, and the training function. Hidden layers are the layers between the input layer and the output layer, where artificial neurons take in a set of weighted inputs and produce an output through an activation function. It is a typical part of nearly any neural network in which engineers emulate the types of activity that go on in the human brain. While stacking many hidden layers allows us to learn more complex relationships in the data, this approach is also more prone to potentially overfitting data. In addition, a validation data set is a data set of the samples used to provide an unbiased evaluation of a model fit on the training data set while tuning model hyperparameters. The difference between the validation data set and the test data set is generally what is used to evaluate competing models. The validation data set is used to compare their performances, whereas the test data set is used to provide an unbiased evaluation of a final model fit on the training data set. Here, we calculated the mean square error (MSE) by the following equation:

$$\mathrm{MSE} = \frac{1}{n}\sum_{i}^{n}(y_i - (\widehat{y_i}))^2 \tag{2}$$

where the desired neural network output is denoted by y_i and the neural network output is denoted by $\widehat{y_i}$ to compare the performance of the trained network for the following variations of two different hyperparameters: 1) the number of hidden layers and 2) the three training functions (the Levenberg–Marquardt, Bayesian regularization, and Scaled conjugate gradient). The number of epochs is also one of the hyperparameters of gradient descent that controls the number of complete passes through the training data set. In other words, an epoch is one learning cycle where the learner sees the whole training data set. A sufficient number of epochs (1000) were used along with each network to guarantee the minimization of the training MSE. Fig. 5(a) shows the calculated MSE of the validation data corresponding to the number of hidden layers and Fig. 5(b) shows the MSE of the test data corresponding to the number of hidden layers from 5 to 15. In Fig. 5(b), MSE with the Bayesian regularization function is always zero because of the function that performs Bayesian regularization BP, which disables the validation stops by default. In other words, this function does not require a validation data set at the point of checking validation to see if the error on the validation set gets better or worse as training goes on. Since the value of the MSE is good when it is close to 0, the number of hidden layers used for the neural network should be ten for this application when using the Levenberg–Marquardt and Bayesian regularization functions. Throughout this article, we used the following data partitioning methods that have been suggested in most of the related articles: 70% of the entire data set for training, 15% of the entire data set for validation, and 15% of the entire data set for testing.

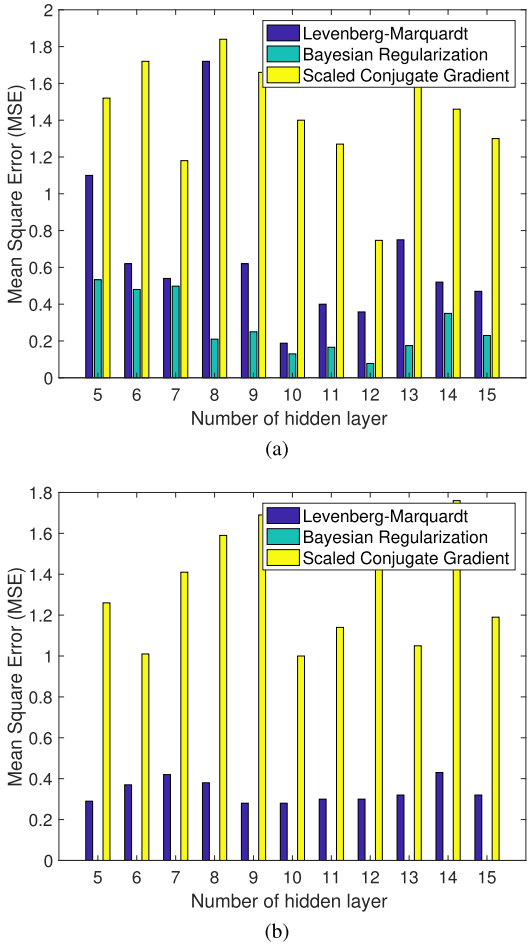

Fig. 5. (a) MSE of the test data. (b) MSE of the validation data.

B. Feedforward Neural Network With Backpropagation

The feedforward neural network also called deep feedforward network is one of the deep learning models. To approximate some function $f(x)$ through the feedforward neural network, when x is the input, the feedforward neural network defines a mapping function $y = f(x;\theta)$ and determines the parameters θ, which gives the best function approximation results [13]. Moreover, the BP method provides a neural network with a set of input values for which the correct output value is known beforehand. In this network, as shown in Fig. 6, the information moves in both directions from the input layers with an associated weight factor (w) to the output layers, while the hidden layers are usually used for improving mapping ability. In this work, we propose a WPT scheme with a three cascading L-type stage impedance-matching network based on a feedforward neural network, which is a similar approach used in [11]. They developed a mapping relationship between the impedance of the equivalent load ($Z_{\text{eq}} = R_{\text{eq}} + jX_{\text{eq}}$) and the matched capacitor set composed of (C_1, C_2) in their Γ-type of matching network. In this work, in consideration of each switch connected to each L-type stage of the matching network, the final output set is composed of (C_1, C_2, C_3). The data set for training to produce a function describing the network consists of the distribution of $|S_{11}|$ values when using the matching network to match impedances within the range of 0 to 20 Ω for R_{eq} and -50 to 50 for X_{eq} with 1-Ω interval in total with a set of 2121 data. The reason to use these dynamic variation ranges of the impedance is based on the consideration of matching the range from small to large impedance variations in real time. In a previously reported work, we proposed the advanced approach using a shallow neural network to classify patterns. Through classification, an automated system declares that the input object belongs to a particular category. A set of 2121 values of the output parameters, which represents the capacitances' values, (C_1, C_2, C_3) from the above trained model acts as the input to select the proper "optimal" single transmitter coil among T_{x1}, T_{x2}, and T_{x3}. After that, the trained classifier can recognize the three categories associated with each set of input parameters. In this work, the selection of

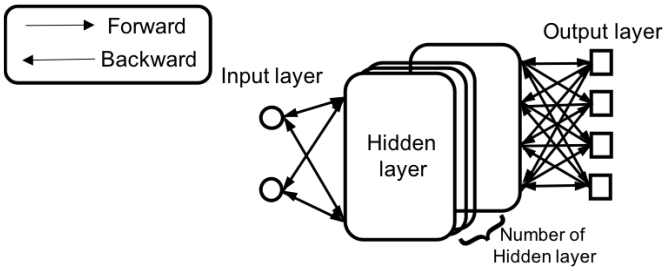

Fig. 6. Schematic of the feedforward neural network with BP.

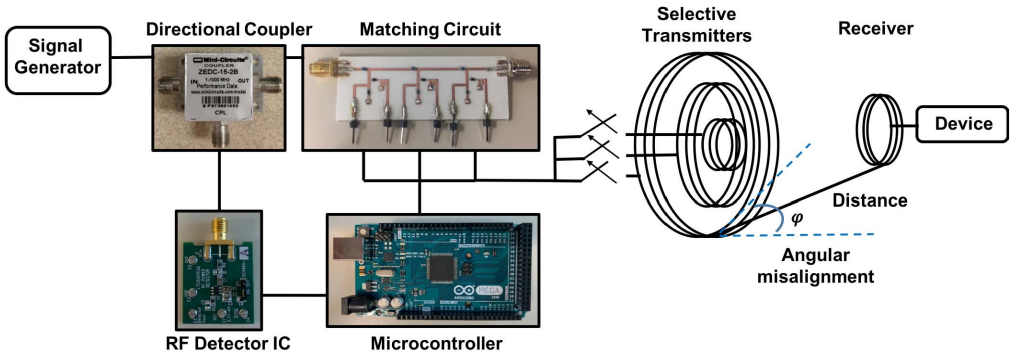

Fig. 7. Block diagram of the proposed real-time range-adaptive impedance-matching WPT system.

the proper transmitter coils among T_{x1}, T_{x2}, and T_{x3} is also included in the output parameter set in consideration of further implementation.

IV. Implementation and Performance Evaluation

A. Implementation of the Proposed System

Firstly, the trained feedforward neural network model is built by the process discussed in Sections III-A and III-B. To predict the capacitance values and classify the type of the transmitter, a training process using the feedforward neural network was implemented. We implemented the trained neural network by extracting layer/output weight factors from the MATLAB simulation as the development of the network on Arduino would be the slower process in terms of training time. Before matching, the initial input impedance of Rx–Tx at 13.56 MHz was measured by a vector network analyzer and shown in Fig. 8. To verify the fabricated three transmitter coil prototypes and the effect of their selective operability, Fig. 8 also shows the measurement results when one of three transmitter coils was manually selected to achieve impedance matching only utilizing the proposed matching circuit depending on each coil-to-coil distance. From these figures, it can be easily deduced that the classified output parameters, capacitance values (C_1, C_2, C_3), is not accurate at certain impedance values, because the trained neural network model assumed strong underlying relationship between those impedances and other transmitter coils. This can be the reason why the S_{11} is high at 15 cm in Fig. 8(a) and at 14 cm in Fig. 8(c), and can be prevented by using selective multi transmitters. As discussed in [6], the coil's matching is improved throughout most of the coil-to-coil distance ranges such as of Rx–Tx1 at 10–14 cm, Rx–Tx2 at 15–19 cm, and Rx–Tx3 at 20–25 cm. Finally, by combining the selective multi transmitters that are controlled automatically, the performance of the proposed approach will be discussed in Section IV-B.

B. Operation Test and Performance Evaluation

To verify the prediction capability for each set of capacitance values of the impedance-matching circuit and the coil selection capability for multicoil transmitters, the performance of the entire real-time range-adaptive matching system was tested and the configuration is shown in Fig. 7. Initially, the S_{11} signal was measured by utilizing a directional coupler, ZEDC-15-2B from Mini-Circuits and the RF detector IC, LTC5507 from the Linear Technology Cooperation. Then, the output dc voltage was measured by utilizing an analog-to-digital (ADC) converter in the microcontroller module not only to calculate the matched capacitor set but also to predict the "optimum" transmitter coil through the neural network. Finally, the Arduino processor outputs the pulsewidth modulation (PWM) signal to drive the voltage that adjusted the capacitance values and controlled the three switches' status in the transmitter selection. To verify the validity of the proposed WPT system, the received power at different separation distances was first measured by using a real-time spectrum analyzer, RSA3408 from Tektronix, Inc., with a tunable matching circuit and multiple Tx coils. The S-parameters of the matched state automatically chosen by the trained neural network model at different coil separation distances were measured by utilizing a vector network analyzer, and the extracted values of S_{21} were used to calculate the PTE expressed in the following equation:

$$\text{PTE} = |S_{21}|^2 \times 100(\%). \tag{3}$$

To verify and validate the proposed approach, Fig. 10 shows the calculated values of PTE at each distance within the range of 10–25 cm comparing the performance when using only one specific Tx coil and with selective Tx coils under the condition of the similar matching approach in [6]. After matching through the trained neural network model, it can be easily seen that the input impedance matching is improved over the entire separation distance range. By utilizing the selective Tx coils, the PTE was more stable and able to avoid the sudden drop at certain distance ranges for two different environments [the capacitance values and the selected single transmitter coil extracted from the trained neural network model based on the simulation results combined with the manually measured result of the tunable matching circuit, and the multi transmitter coils, respectively (Case 1) and automatically measured results of the entire real-time range adaptive system (Case 2)]. Especially, at distances 12, 13, 14, 16, 18, 19, and 22 cm, the capacitance values and the selected single transmitter coil extracted from the trained neural network model result in a significant improvement, as clearly shown in Fig. 9. Moreover, the proposed approach achieves a PTE

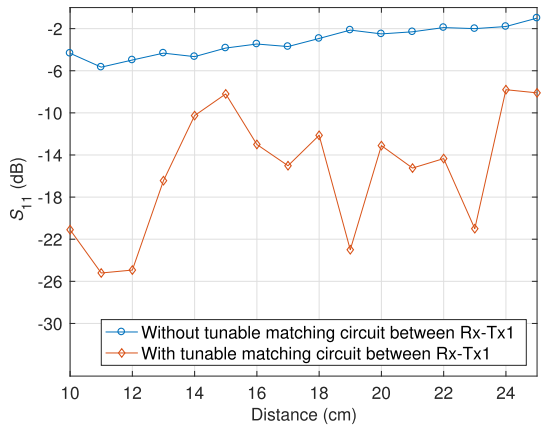

(a)

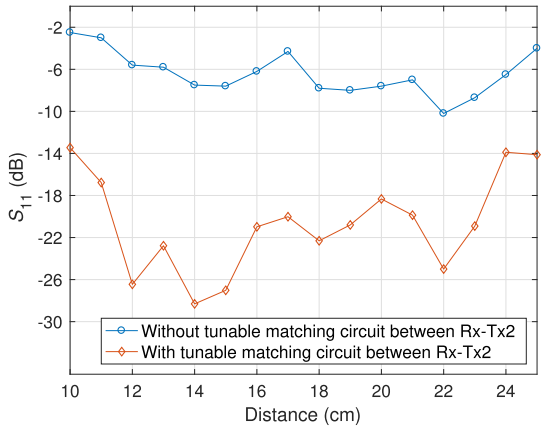

(b)

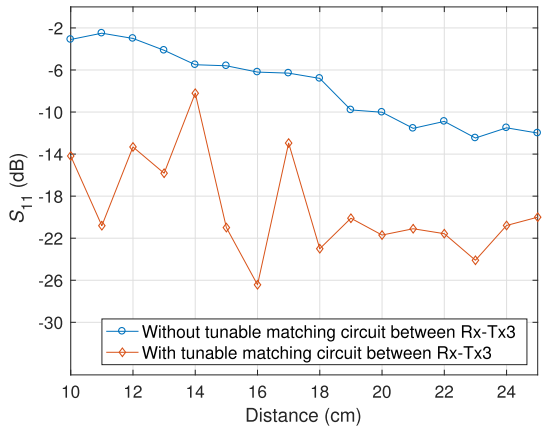

(c)

Fig. 8. (a) Measured values of the reflection coefficient (S_{11}) only with Rx–Tx1. (b) Measured values of the reflection coefficient (S_{11}) only with Rx–Tx2. (c) Measured values of the reflection coefficient (S_{11}) only with Rx–Tx3.

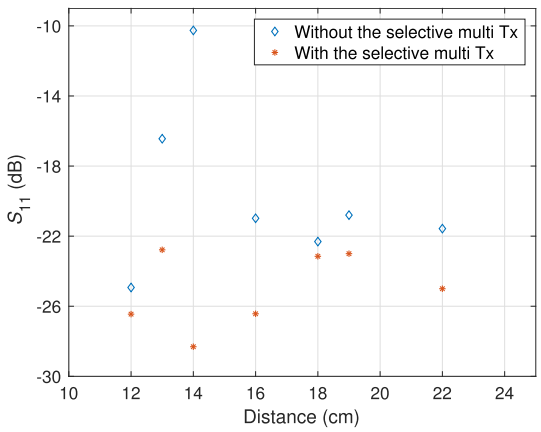

Fig. 9. Transmitter coil selectivity effect.

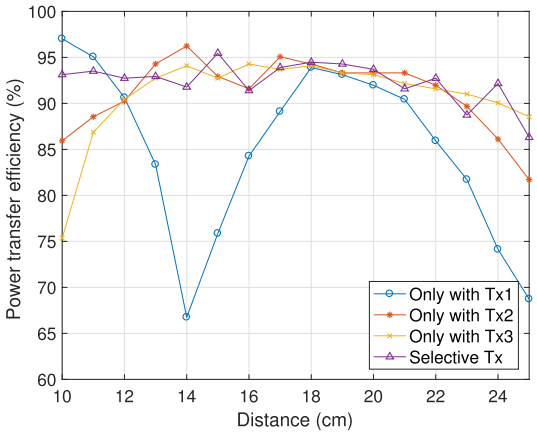

(a)

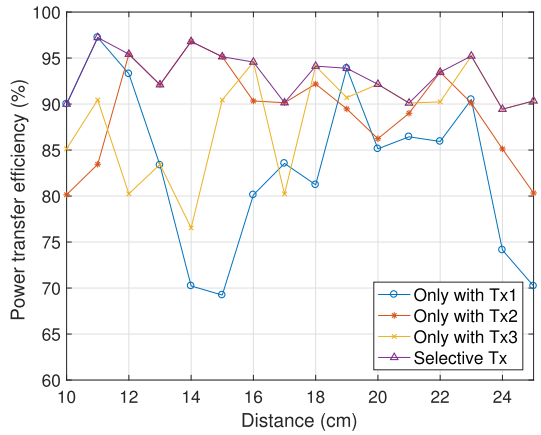

(b)

Fig. 10. (a) PTE without the selective Tx versus with the selective Tx in Case 1. (b) PTE without the selective Tx versus with the selective Tx in Case 2.

of around 90% over the distance range within 10–25 cm. In angular coil misalignment environment, the plane of the Tx coil is tilted to form an angle in $-30°$ and $30°$ along ϕ angle at 10, 15, and 20 cm, as shown in Fig. 7, and the system input impedance matching is improved, as shown in the Smith chart in Fig. 11. It can be easily seen that the matching results by the proposed method even in angular coil misalignment environment are concentrated at the center of the Smith chart, which is close to target impedance 50 Ω.

To identify the performance of the range-adaptive impedance-matching system and show the limitation of existing techniques, a comparison table is shown in Table II. Compared with the previous work utilizing GA [10], the significant improvement in the operation range while retaining high PTE was confirmed, with a smaller number of stages resulting in a reduced loss associated with the lumped circuit. Compared with the WPT system configuration in [9] that employed

TABLE II
COMPARISON OF REPORTED RANGE-ADAPTIVE WPT SYSTEMS

	$\|S_{11}\|$ measurement for automatic matching	Tx-Rx structure	Type of matching circuit	Tuning method	Algorithm type/speed	Operation range(cm) over 80% of PTE
[7]	Directional coupler rectifier	Two resonators	L-type network in Tx	Relays (Switching capacitors)	Decent search with scaling,<1.5s	9-21
[8]	Rectifiers	Four resonators	π-type network in both Tx and Rx	Switching capacitors	Parasitic and conjugate match, -	10-22
[9]	Directional coupler rectifier	Four resonator resonators	Shunt network in both Tx and Rx	Relays (Switching capacitors) varactors, multi-loop	Searching algorithm, <1.2s	10-40
[10]	Directional coupler RF detector IC	Two resonators	Cascading 6 L-type network in Tx	p-i-n diodes (Switching capacitors)	Genetic algorithm, <0.064s	10-16
[11]	Directional coupler RF detector IC	Four resonators	Γ-type network in Tx	Stepper motors for capacitors	Neural network, <0.063s	0-20
This work	Directional coupler RF detector IC	Two resonators	Cascading 3 L-type network in Tx	Tunable capacitors p-i-n diodes, multi-coil Tx	Neural network, <0.063s	10-25

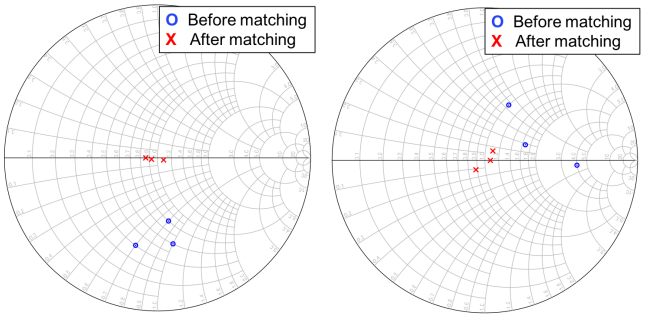

(a) (b)

Fig. 11. Smith chart of the input impedance values of the system at distances of 10, 15, and 20 cm for an angular misalignment of (a) -30° along ϕ angle and (b) $+30^\circ$ along ϕ angle.

the variable capacitances for the tunable matching circuit and selective multiloop to reduce the variation in the input impedance, the proposed WPT system utilizing the neural network is more suitable for applications in terms of speed, which is the major limitation for fast real-time operation. Moreover, this work reveals the remarkable PTE enhancement over the entire separation distance range that can be achieved with the selective multi transmitters when compared with [11] in addition to the tunable matching circuit utilizing the neural network algorithm.

V. CONCLUSION

This work describes the implementation of an ML strategy based on the neural network for real-time range-adaptive automatic impedance matching of WPT applications. In this article, range-adaptive impedance matching of the WPT system utilizing neural network algorithms was demonstrated. The implementation of the feedforward neural network and pattern recognition techniques for real-time range-adaptive automatic impedance matching of WPT applications can not only predict the capacitance value of the matching circuit under a specific environment but also select one of the Tx coils that maximize the Rx–Tx PTE up to 95%. In addition, the proposed model is generalizable to contexts such as misalignment of Rx–Tx coils and a wide range of operation distances. The work reported here could greatly enhance the state-of-the-art real-time range-adaptive automatic impedance-matching techniques in the WPT system.

REFERENCES

[1] A. P. Sample, D. T. Meyer, and J. R. Smith, "Analysis, experimental results, and range adaptation of magnetically coupled resonators for wireless power transfer," *IEEE Trans. Ind. Electron.*, vol. 58, no. 2, pp. 544–554, Feb. 2011.
[2] W. Fu, B. Zhang, and D. Qiu, "Study on frequency-tracking wireless power transfer system by resonant coupling," in *Proc. IEEE 6th Int. Power Electron. Motion Control Conf.*, May 2009, pp. 2658–2663.
[3] T. P. Duong and J.-W. Lee, "Experimental results of high-efficiency resonant coupling wireless power transfer using a variable coupling method," *IEEE Microw. Wireless Compon. Lett.*, vol. 21, no. 8, pp. 442–444, Aug. 2011.
[4] G. Lee, B. H. Waters, Y. G. Shin, J. R. Smith, and W. S. Park, "A reconfigurable resonant coil for range adaptation wireless power transfer," *IEEE Trans. Microw. Theory Techn.*, vol. 64, no. 2, pp. 624–632, Feb. 2016.
[5] J. Lee, Y. Lim, H. Ahn, J.-D. Yu, and S.-O. Lim, "Impedance-matched wireless power transfer systems using an arbitrary number of coils with flexible coil positioning," *IEEE Antennas Wireless Propag. Lett.*, vol. 13, pp. 1207–1210, 2014.
[6] H. Qiu, Y. Narusue, Y. Kawahara, T. Sakurai, and M. Takamiya, "Digital coil: Transmitter coil with programmable radius for wireless powering robust against distance variation," in *Proc. IEEE Wireless Power Transf. Conf. (WPTC)*, Montreal, QC, Canada, Jun. 2018, pp. 1–4.
[7] T. C. Beh, M. Kato, T. Imura, S. Oh, and Y. Hori, "Automated impedance matching system for robust wireless power transfer via magnetic resonance coupling," *IEEE Trans. Ind. Electron.*, vol. 60, no. 9, pp. 3689–3698, Sep. 2013.
[8] B. H. Waters, A. P. Sample, and J. R. Smith, "Adaptive impedance matching for magnetically coupled resonators," in *Proc. Prog. Electromagn. Res. Symp.*, Aug. 2012, pp. 694–701.
[9] J. Kim and J. Jeong, "Range-adaptive wireless power transfer using multiloop and tunable matching techniques," *IEEE Trans. Ind. Electron.*, vol. 62, no. 10, pp. 6233–6241, Oct. 2015.
[10] J. Bito, S. Jeong, and M. M. Tentzeris, "A real-time electrically controlled active matching circuit utilizing genetic algorithms for wireless power transfer to biomedical implants," *IEEE Trans. Microw. Theory Techn.*, vol. 64, no. 2, pp. 365–374, Feb. 2016.
[11] Y. Li, W. Dong, Q. Yang, J. Zhao, L. Liu, and S. Feng, "An automatic impedance matching method based on the feedforward-backpropagation neural network for a WPT system," *IEEE Trans. Ind. Electron.*, vol. 66, no. 5, pp. 3963–3972, May 2019.
[12] S. Jeong, T.-H. Lin, and M. M. Tentzeris, "Range-adaptive impedance matching of wireless power transfer system using a machine learning strategy based on neural networks," in *IEEE MTT-S Int. Microw. Symp. Dig.*, Boston, MA, USA, Jun. 2019, pp. 1423–1425.
[13] K.-I. Funahashi, "On the approximate realization of continuous mappings by neural networks," *Neural Netw.*, vol. 2, no. 3, pp. 183–192, 1989.

Soyeon Jeong (S'14) received the B.S. degree in electrical engineering from Gangneung–Wonju National University, Gangneung, South Korea, in 2010, and the M.E. degree in electrical and computer engineering from the Georgia Institute of Technology, Atlanta, GA, USA, in 2014, where she is currently pursuing the Ph.D. degree with the Agile Technologies for High-Performance Electromagnetic Novel Applications (ATHENA) Group.

She is involved in the entire system of wireless power transfer (WPT) on methods, sensor component design, high-frequency characterization and environmental testing to the design, and the simulation and fabrication of the RF system embedding the sensor. Her current research interests include the applications of machine learning (ML) strategy for WPT and identification.

Tong-Hong Lin (GS'18) received the B.S.E.E. and M.S. degrees from National Taiwan University, Taipei, Taiwan, in 2011 and 2013, respectively. He is currently pursuing the Ph.D. degree in electrical and computer engineering and the M.S. degree in computational science and engineering at the Georgia Institute of Technology, Atlanta, GA, USA.

He is currently a Research Assistant with the ATHENA Group, 3-D Systems Packaging Research Center, Georgia Institute of Technology. His current research interests include characterization of inkjet printing and 3-D printing materials and fabrication processes, application of inkjet printing and 3-D printing to wearable and flexible electronics, RF energy harvesting systems, wireless power transfer systems, wireless sensing networks, antenna-in-package design, 5G system-on-package modules, and glass packaging design.

Mr. Lin was a recipient of the Student Travel Award of the 2018 Electronic Components and Technology Conference (ECTC).

Manos M. Tentzeris (S'89–M'92–SM'03–F'10) received the Diploma degree *(magna cum laude)* in electrical and computer engineering from the National Technical University of Athens, Athens, Greece, in 1992, and the M.S. and Ph.D. degrees in electrical engineering and computer science from the University of Michigan, Ann Arbor, MI, USA, in 1993 and 1998, respectively.

He was a Visiting Professor with the Technical University of Munich, Munich, Germany, in 2002, GTRI-Ireland, Athlone, Ireland, in 2009, and LAAS-CNRS, Toulouse, France, in 2010. He has served as the Head of the GT-ECE Electromagnetics Technical Interest Group, as the Georgia Electronic Design Center Associate Director of the RFID/Sensors Research, as the Georgia Tech NSF-Packaging Research Center Associate Director of the RF Research, and as the RF Alliance Leader, Georgia Institute of Technology, Atlanta, GA, USA, where he currently heads the Agile Technologies for High-Performance Electromagnetic Novel Applications (ATHENA) Research Group (20 researchers).

He is also a Ken Byers Professor of flexible electronics with the School of Electrical and Computer Engineering, Georgia Institute of Technology. He has authored more than 650 articles in refereed journals and conference proceedings, 5 books, and 25 book chapters. He holds 14 patents. He has given more than 100 invited talks to various universities and companies all over the world. He has helped develop academic programs in 3-D/inkjet-printed RF electronics and modules, flexible electronics, origami and morphing electromagnetics, highly integrated/multilayer packaging for RF and wireless applications using ceramic and organic flexible materials, article-based RFIDs and sensors, wireless sensors and biosensors, wearable electronics, green electronics, energy harvesting and wireless power transfer (WPT), nanotechnology applications in RF, microwave MEMS, and SOP-integrated (ultra-wideband, multiband, mmW, and conformal) antennas.

Dr. Tentzeris is a member of the URSI-Commission D, the MTT-15 Committee, and the Technical Chamber of Greece, an Associate Member of the EuMA, and a Fellow of the Electromagnetic Academy. He was a recipient or corecipient of the 1997 Best Paper Award from the International Hybrid Microelectronics and Packaging Society, the 2000 NSF CAREER Award, the 2001 ACES Conference Best Paper Award, the 2002 International Conference on Microwave and Millimeter-Wave Technology Best Paper Award, Beijing, China, the 2002 Georgia Tech-ECE Outstanding Junior Faculty Award, the 2003 NASA Godfrey Art Anzic Collaborative Distinguished Publication Award, the 2003 IBC International Educator of the Year Award, the 2003 IEEE CPMT Outstanding Young Engineer Award, the 2004 IEEE TRANSACTIONS ON ADVANCED PACKAGING Commendable Paper Award, the 2006 IEEE MTT-S Outstanding Young Engineer Award, the 2006 Asia–Pacific Microwave Conference Award, the 2007 IEEE AP-S Symposium Best Student Paper Award, the 2007 IEEE MTT-S IMS Third Best Student Paper Award, the 2007 ISAP 2007 Poster Presentation Award, the 2009 IEEE TRANSACTIONS ON COMPONENTS AND PACKAGING TECHNOLOGIES Best Paper Award, the 2009 E. T. S. Walton Award from the Irish Science Foundation, the 2010 IEEE Antennas and Propagation Society Piergiorgio L. E. Uslenghi Letters Prize Paper Award, the 2010 Georgia Tech Senior Faculty Outstanding Undergraduate Research Mentor Award, the 2011 International Workshop on Structural Health Monitoring Best Student Paper Award, the 2012 FiDiPro Award in Finland, the iCMG Architecture Award of Excellence, the 2013 *IET Microwaves, Antennas and Propagation* Premium Award, the 2014 Georgia Tech ECE Distinguished Faculty Achievement Award, the 2014 IEEE RFID-TA Best Student Paper Award, the 2015 *IET Microwaves, Antennas and Propagation* Premium Award, the 2016 Bell Labs Award Competition 3rd Prize, the 2017 Georgia Tech Outstanding Achievement in Research Program Development Award, and the 2017 Archimedes IP Salon Gold Medal. He was the TPC Chair of the IEEE MTT-S IMS 2008 Symposium and the Chair of the 2005 IEEE CEM-TD Workshop. He is also the Vice Chair of the RF Technical Committee (TC16) of the IEEE CPMT Society. He is also the founder and the Chair of the RFID Technical Committee (TC24) of the IEEE MTT-S and the Secretary/Treasurer of the IEEE C-RFID. He served as the IEEE MTT-S Distinguished Microwave Lecturer from 2010 to 2012 and the IEEE CRFID Distinguished Lecturer. He is also an Associate Editor of the IEEE TRANSACTIONS ON MICROWAVE THEORY AND TECHNIQUES, the IEEE TRANSACTIONS ON ADVANCED PACKAGING, and *International Journal of Antennas and Propagation*.